OPEN

Original article

Nuclear Medicine Communications

Comparison of ^{68}Ga-FAPI-04 and fluorine-18-fluorodeoxyglucose PET/computed tomography in the detection of ovarian malignancies

Wenlu Zheng[a,b,c,d,e,f], Lin Liu[c,d,e,f], Yue Feng[c,d,e,f], Li Wang[c,d,e,f] and Yue Chen[a,c,d,e,f]

Background **Currently, fluorine-18-fluorodeoxyglucose (^{18}F-FDG) is the most frequently used diagnostical radiotracer for PET/computed tomography (PET/CT) in ovarian malignancies. However, ^{18}F-FDG has some limitations. The fibroblast activation protein inhibitor (FAPI) previously demonstrated highly promising results in studies on various tumor entities and ^{68}Ga-labeled FAPI presents a promising alternative to ^{18}F-FDG. This study aimed to compare the performance of ^{68}Ga-FAPI and ^{18}F-FDG PET/CT for imaging of ovarian malignancies.**

Methods **A total of 27 patients were included in this retrospective study conducted at the Affiliated Hospital of Southwest Medical University between June 2020 and February 2022. The ^{18}F-FDG and ^{68}Ga-FAPI uptakes of tumors, lymph nodes, and distant metastases were quantified using the maximum standardized uptake values, and the tumor-to-background ratios were also evaluated and calculated by using the Wilcoxon signed-rank test.**

Results **Twenty-one patients with suspected (n=11) and previously treated ovarian malignancies (n=10) were in statistical analysis finally. For detecting tumors, ^{68}Ga-FAPI PET/CT was more sensitive than ^{18}F-FDG PET/CT [14 of 14 (100%) vs. 11 of 14 (78%)], lymph node metastases [75 of 75 (100%) vs. 60 of 75 (80%)] and superior to ^{18}F-FDG PET/CT in terms of the peritoneal and pleural metastases [9 of 9 (100%) vs. 5 of 9 (56%)]. For four of the newly diagnosed patients (n=11), ^{68}Ga-FAPI PET/CT upstaged the clinical stage compared to ^{18}F-FDG PET/CT.**

Conclusion **^{68}Ga-FAPI PET/CT has superior potential in the detection of ovarian cancers, especially in peritoneal carcinomatosis. ^{68}Ga-FAPI PET/CT may be a promising supplement for staging and follow-up of ovarian malignancies. *Nucl Med Commun* 44: 194–203 Copyright © 2022 The Author(s). Published by Wolters Kluwer Health, Inc.**

Nuclear Medicine Communications 2023, **44**:194–203

Keywords: fluorine-18-fluorodeoxyglucose, ^{68}Ga-FAPI-04, ovarian malignancies, fibroblast activating protein, PET/computed tomography

[a]Faculty of Chinese Medicine, Macau University of Science and Technology, [b]State Key Laboratory of Quality Research in Chinese Medicine (Macau University of Science and Technology), Macau, [c]Department of Nuclear Medicine, The Affiliated Hospital, Southwest Medical University, [d]Nuclear Medicine and Molecular Imaging Key Laboratory of Sichuan Province, [e]Institute of Nuclear Medicine, Southwest Medical University and [f]Academician (Expert) Workstation of Sichuan Province, Luzhou, China

Correspondence to Yue Chen, MD, Department of Nuclear Medicine, The Affiliated Hospital, Southwest Medical University, Luzhou, China
Tel: +86 830 3165720; e-mail: chenyue5523@126.com

Received 13 September 2022 **Accepted** 15 November 2022.

Introduction

Ovarian malignancies are the most frequent cancer-associated deaths of female reproductive organs. Poor outcomes are associated with them, as they are usually detected at an advanced stage [1]. The pathological types of primary ovarian malignancies are mainly classified into two groups: epithelial and non-epithelial. Among them, 95% of ovarian cancer originates from ovarian epithelial cells called epithelial ovarian cancer (EOC). High-grade serous carcinomas (HGSC) account for up to 70% of EOC while low-grade serous carcinomas (LGSC) up to 5%, and the other three primary histological types of EOC are endometrioid, mucinous, and clear cell [2]. Initial therapy includes primary debulking surgery and chemotherapy [3]. Secondary ovarian malignancies usually occur from gastrointestinal cancer, for example, sigmoid cancer, gastric cancer, and carcinoid of appendix. Non-specific symptoms of the abdomen, late diagnosis, and high metastatic rate often lead to a high death rate. Therefore, a reliable imaging tool for diagnosis and precise staging is of the essence [4]. Fluorine-18-fluorodeoxyglucose (^{18}F-FDG) is the widely used molecular imaging modality for oncological malignancies which reflects glucose metabolism in glucose-consuming tissues [5,6]. Some limitations; however, must be taken into account. First, the accumulation of ^{18}F-FDG is influenced by different histological types of cancer such as ovarian mucinous carcinoma. Further, ^{18}F-FDG PET/computed tomography (CT) has limited utility for staging lymph nodes and distant metastases in ovarian cancer due to low sensitivity and high physiological background activity in the

abdominal cavity. Moreover, physiologic accumulation of ovaries can result in false-positive ovaries uptake of ^{18}F-FDG [7,8]. Recently, a novel radiotracer, the fibroblast activation protein inhibitor (FAPI) has shown promising results in various tumor entities targeting the fibroblast activation protein (FAP). Cancer-associated fibroblasts that are part of the stroma of many tumors express FAP [9,10]. There is some evidence to suggest that ^{68}Ga-FAPI PET/CT might be superior to ^{18}F-FDG-PET/CT for ovarian cancer, based on previous studies [11]. Studies that comprehensively evaluate ^{68}Ga-FAPI PET/CT for ovarian cancer remain lacking. In this study, we compared the detection of ^{68}Ga-FAPI PET/CT and ^{18}F-FDG PET/CT in the tumor, lymph node metastases, distant metastases in ovarian malignancies.

Materials and methods

Patients selection

A total of 27 patients with ovarian malignancies who underwent ^{68}Ga-FAPI and ^{18}F-FDG PET/CT were retrospectively analyzed at the Affiliate Hospital of Southwest Medical University from June 2020 to February 2022 (ethics committee approval no. 2020035). A written informed consent form was signed by all patients. The inclusion criteria were as follows: (a) aged 18 or older;(b) suspected, newly diagnosed, or previously treated ovarian cancer; (c) patients who underwent paired ^{18}F-FDG PET/CT and ^{68}Ga-FAPI PET/CT to determine the most appropriate treatment strategy based on tumor staging. Exclusion criteria were as follows: (a) in the case of pregnant patients; (b) patients receiving treatment including surgery, chemotherapy, radiotherapy, and targeted therapy less than 3 months before underwent ^{68}Ga-FAPI or ^{18}F-FDG PET/CT, and (c) an inability or unwillingness to provide written informed consent. After ^{18}F-FDG PET/CT, ^{68}Ga-FAPI PET/CT was performed in less than 1 week.

Radiopharmaceuticals and PET imaging

A ^{18}F-FDG synthesis module was used in our laboratory to produce ^{18}F-FDG according to the standard method (PET Science and Technology). The FAPI precursor (1, 4, 7, 10-tetraazacyclododecane-1, 4, 7, 10-tetraacetic acid-containing ligand FAPI-04) was purchased from MedChemExpress (New Jersey, USA). ^{68}Ga-FAPI was radiolabeled and purified as previously described [12]. ^{68}Ga-FAPI had a radiochemical purity of >98% as determined by radio-high-performance liquid chromatography. Overall, the ^{18}F-FDG and ^{68}Ga-FAPI products were sterile and pyrogen-free and meet all set criteria before use.

18F-FDG imaging

Before undergoing 18F-FDG PET/CT, patients were instructed to fast for at least six hours, and their serum blood glucose levels were measured before they were injected with ^{18}F-FDG to ensure that they were within the normal range (<150 mg/dL). The intravenous dose of ^{18}F-FDG was 3.7 MBq/kg (0.1 mCi/kg) [13].

^{68}Ga-FAPI imaging

^{68}Ga-FAPI was prepared in accordance with a previous protocol. ^{68}Ga-FAPI was injected intravenously at a dose of 1.85–3.7 MBq/kg (0.05–0.1 mCi/kg).

The PET/CT scan was performed approximately 45–60 min after intravenous administration (uMI780; United Imaging Healthcare, Shanghai, China). The CT parameters were as follows: tube voltage, 120 kV; current, 120 mA; slice thickness, 3.00 mm. PET images were acquired during PET at both sites (from the brain to the upper thigh). PET images of ^{18}F-FDG and ^{68}Ga-FAPI were acquired at 1.5 and 3.0 min/bed, respectively. Postprocessing Workstation (uWS-MI, version R002; United Imaging Healthcare) was used to reconstruct PET data using an ordered subset expectation (OSEM; United Imaging Healthcare).

PET/computed tomography image evaluation

The ^{68}Ga-FAPI and ^{18}F-FDG PET/CT images were evaluated by two board-certified nuclear medicine physicians. Any differences in opinion were resolved by consensus. In order to avoid any bias, the blind method was applied when the two physicians evaluated the images from different tracers. Tracer uptakes in ovarian tumor lesions, lymph nodes, and distant metastases, which were higher than that of adjacent background tissues were included in this study. Moreover, the semi-quantitative parameters were calculated using the maximum standardized uptake values (SUVmax). The tumor-to-background ratios (TBRs) were also calculated to quantify image contrast. TBR was calculated by dividing the SUVmax of the primary tumor and metastases by background values (SUVmean). Peritoneal, mesentery, and omentum metastases were classified as peritoneal carcinomatosis. All ovarian tumor lesions were confirmed with pathological biopsies and surgeries. Nevertheless, the lymph nodes and distant metastasis involved were not possible to obtain pathological results all. Therefore, the pathological biopsies, surgical resection, and imaging follow-up results (ultrasound, CT, MRI, bone scan) were all considered as reference standards. The time of the follow-up was at least 3 months.

Statistical analysis

All statistical analyses were performed using IBM SPSS Statistics software for Windows version 26.0 (IBM, Chicago, USA). We performed descriptive analyses of all patients including demographic and tumor-specific characteristics. The median and SD were used for the determination of SUVmax and TBR. The uptakes of ^{18}F-FDG and ^{68}Ga-FAPI were compared by using the Wilcoxon signed-rank test. The ^{68}Ga-FAPI SUVmax between inflammatory and Ovarian malignancies was compared

using the Mann–Whitney *U* test. A two-tailed $P < 0.05$ was considered to indicate a statistically significant difference.

Results

Patient characteristics

This study consisted of 27 female patients with suspected and previously treated ovarian malignancies. The study design is presented in Fig. 1. Seventeen patients underwent PET/CT for initial tumor assessment. Among them, 11 were newly diagnosed with EOC. Ten of the 27 patients who underwent PET/CT for restaging had tumor recurrence from previous partially resected lesions. Of them, three patients were diagnosed with ovarian tuberculosis, the other three were confirmed to have secondary ovarian malignancies originating from gastric signet-ring cell carcinoma ($n = 1$), appendix mucinous carcinoma ($n = 1$), and cervical adenocarcinoma ($n = 1$). The patient characteristics are presented in Table 1. Finally, 21 patients who were diagnosed with primary ovarian malignancies for staging and restaging were involved in the statistical analysis. All patients tolerated ^{18}F-FDG and ^{68}Ga-FAPI PET/CT, and none reported any adverse effects related to ^{68}Ga-FAPI.

Comparison of ^{18}F-FDG and ^{68}Ga-FAPI PET/computed tomography in primary ovarian tumors

^{68}Ga-FAPI was able to successfully detect all 14 tumors (100%) of which 11 patients were newly diagnosed with primary ovarian malignancies And three of ten patients with postoperative ovarian malignancies for tumor recurrence restaging while ^{18}F-FDG PET/CT helped detect 11 of the 14 tumors (78%). There are three patients including one which diagnosed with a history of high-grade mucinous carcinoma of ovary resection (patient 1, Fig. 2), and two diagnosed with ovarian serous carcinoma that was not diagnosed at ^{18}F-FDG PET/CT but was at ^{68}Ga-FAPI PET/CT. Nevertheless, The SUVmax for ^{68}Ga-FAPI PET/CT was not higher than ^{18}F-FDG PET/CT (median SUVmax, 6.9 vs. 6.8, respectively; $P = 0.57$). Nonetheless, ^{68}Ga-FAPI PET/CT showed a lower background uptake and a higher TBR (median TBR, 5.8 vs. 2.7, respectively; $P < 0.001$) (Table 2).

Comparison of ^{18}F-FDG and ^{68}Ga-FAPI PET/computed tomography in lymph node metastases

Thirteen of the 21 patients were shown to have positive lymph nodes ($n = 76$) on either ^{68}Ga-FAPI or ^{18}F-FDG PET/CT. Four, six, forty-six, and twenty positive lymph nodes were detected in the neck, thorax, abdomen, and pelvis regions, respectively. ^{68}Ga-FAPI PET/CT detected more positive lymph nodes in the neck (4 vs. 3), abdomen (46 vs. 35), and pelvis (20 vs. 18) regions than that with ^{18}F-FDG PET/CT, besides that in the thorax, which was equal (6 vs. 6). Positive lymph nodes were confirmed using pathological examination ($n = 17$), and ultrasound, contrast-enhanced CT, MRI, and follow-up results served as the reference standard ($n = 58$). Seventy-five positive lymph nodes in 13 patients were diagnosed as nodal metastases. Only five patients exhibited lymph node metastases localized in the abdomen region and one exhibited nodal metastases in the pelvic site. Lymph node involvement was correctly diagnosed using ^{68}Ga-FAPI in 75 of 75 (100%) lymph nodes

Fig. 1

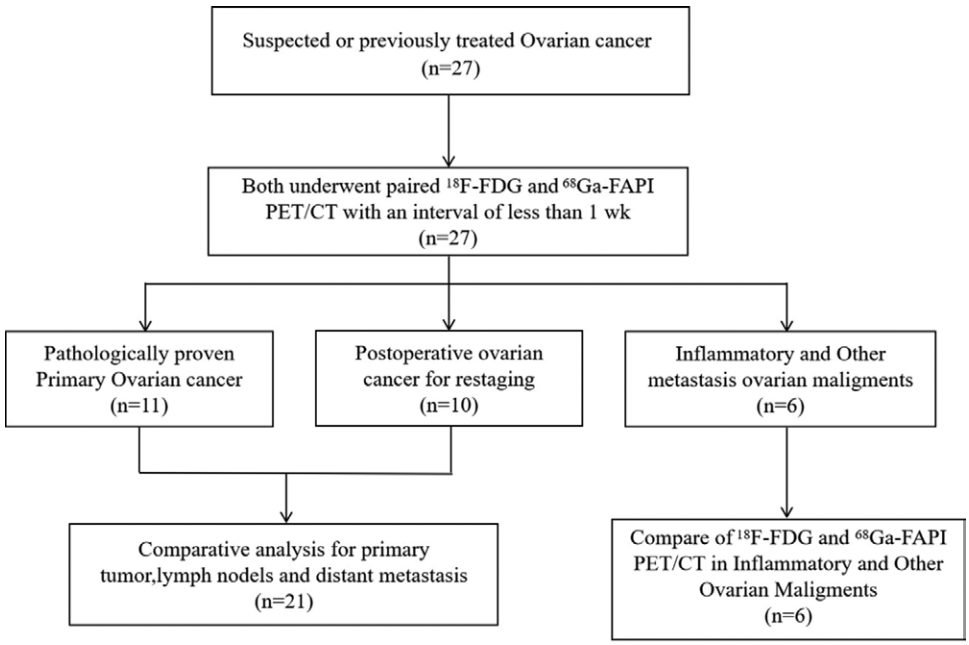

Flow diagram shows patient selection details. ^{18}F-FDG, fluorine-18-fluorodeoxyglucose; ^{68}Ga-FAPI, gallium 68-fibroblast-activated protein inhibitor.

Table 1 Summary of patient characteristics

Characteristic	Value
No. of patients	27
Age (years)[a]	56±12 (35–84)
Indication for PET/CT	
Diagnosis and initial staging	11 (40%)
Primary ovarian malignancies	11
Restaging	10 (37%)
Postoperative ovarian malignancies	10
Histologic findings	
Ovarian primary malignancies	21 (78%)
High-grade serous carcinoma	17
High-grade mucinous carcinoma	1
Low-grade serous carcinoma	3
Secondary ovarian malignancies and ovarian tuberculosis	6 (22%)
Gastric signet-ring cell carcinoma (Krukenberg's tumor)	1
Appendix mucinous carcinoma	1
Cervical adenocarcinoma	1
Ovarian tuberculosis	3

PET/CT, PET/computed tomography.
[a]Age is expressed as the mean±SD, with range in parentheses.

(false-positive uptake in one lymph node); however, 60 of 75 (80%) lymph nodes were diagnosed correctly by using ^{18}F-FDG PET/CT (false-negative uptake in fifteen lymph nodes and false-positive uptake in two lymph nodes). Among the 75 lymph node metastases, 15 (including 1 neck, 11 abdominal, and three pelvic lymph nodes) were missed on ^{18}F-FDG PET/CT. The SUVmax of ^{68}Ga-FAPI was much higher than that of ^{18}F-FDG (median SUVmax, 7.0 vs. 4.4, respectively; $P=0.01$) (Table 2). One lymph node confirmed as reactive in left axilla was misdiagnosed as lymph node metastasis on both ^{68}Ga-FAPI and ^{18}F-FDG PET/CT (Fig. 3). Similarly, one inflammatory lymph node from the right iliac vessel area was misdiagnosed as lymph node metastasis with ^{18}F-FDG PET/CT.

Comparison of ^{18}F-FDG and ^{68}Ga-FAPI PET/computed tomography in distant metastases

Fourteen of the 21 patients diagnosed with distant metastases located in the bone and viscus that were detected using either ^{68}Ga-FAPI or ^{18}F-FDG PET/CT, including 4 bone, 4 liver, and 3 spleen metastases. The bone distant metastases were localized only in one participant (Fig. 1); the spleen distant metastases were also localized in 1 participant (patient 20); the liver metastases were located in 2 patients (Fig. 4) and the other distant metastases were localized in the peritoneal and pleural metastases from 10 patients. Numerous positive metastases were detected and could not be counted (the maximum diameter was greater than 2 cm; Figs 5 and 6). All of the distant metastases were confirmed by pathologic examination and follow-up

Fig. 2

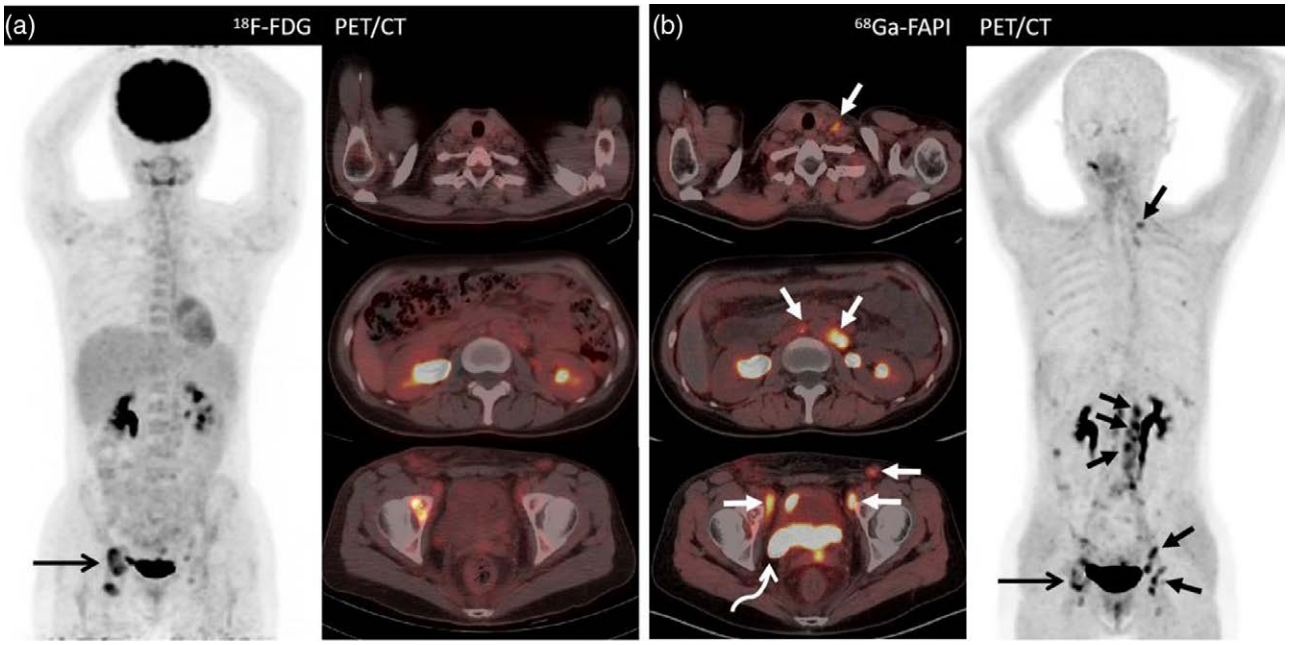

A 35-year-old woman (Patient 1) with a history of poorly differentiated mucinous adenocarcinoma of the ovary resection who underwent fluorine-18-fluorodeoxyglucose (^{18}F-FDG) positron emission tomography/computed tomography (PET/CT) for routine follow-up. Images from both ^{18}F-FDG PET/CT and ^{68}Ga-FAPI PET/CT demonstrate intense uptake in the right ilium. (a) long arrow [maximum standardized uptake value (SUVmax), 6.4]; (b) long arrow (SUVmax, 7.6). Aside from this, ^{18}F-FDG PET/CT images show no abnormal uptake throughout the body (left image: anterior maximum intensity projection image obtained on ^{18}F-FDG PET; right upper image: axial fused PET image of the neck; right middle image: axial fused PET image of the abdomen; right lower image: axial fused PET/CT image of the pelvis). Moreover, the ^{68}Ga-FAPI PET/CT images show a higher uptake in the neck lymph node (short arrow; SUVmax, 4.4) and intense tracer uptake at the retroperitoneal lymph nodes (short arrows; SUVmax, 7.5) and pelvic site of recurrence (bent arrow; SUVmax, 6.9). A subsequent biopsy of the neck nodule shows a metastatic ovarian serous carcinoma. ^{18}F-FDG, fluorine-18-fluorodeoxyglucose; ^{68}Ga-FAPI, gallium 68-labeled fibroblast-activation protein inhibitor; SUVmax, maximum standardized uptake values.

Table 2 Maximum standardized uptake values and tumor-to-background ratio comparison between ^{18}F-FDG and ^{68}Ga-FAPI PET/computed tomography in the primary tumor and nodal and distant metastases

	Median, SUVmax-FDG	Median, SUVmax-FAPI	*P* value	Median, TBR-FDG	Median, TBR-FAPI	*P* value
Primary tumors	6.8	6.9	0.57	2.7	5.8	<0.001
Nodal metastasis	4.4	7.0	0.01	2.2	7.0	<0.001
Bone and visceral metastases	7.4	6.9	0.14	2.4	3.4	0.14
Peritoneal and pleural metastases	7.6	10.1	0.03	3.0	10.1	0.005

P value are for comparison of maximum standardized uptake value (SUVmax) and TBR with ^{18}F-FDG and ^{68}Ga-FAPI.
^{18}F-FDG, fluorine-18-fluorodeoxyglucose; ^{68}Ga-FAPI, gallium 68-labeled fibroblast-activation protein inhibitor; SUVmax, maximum standardized uptake value; TBR, tumor to background ratio.

Fig. 3

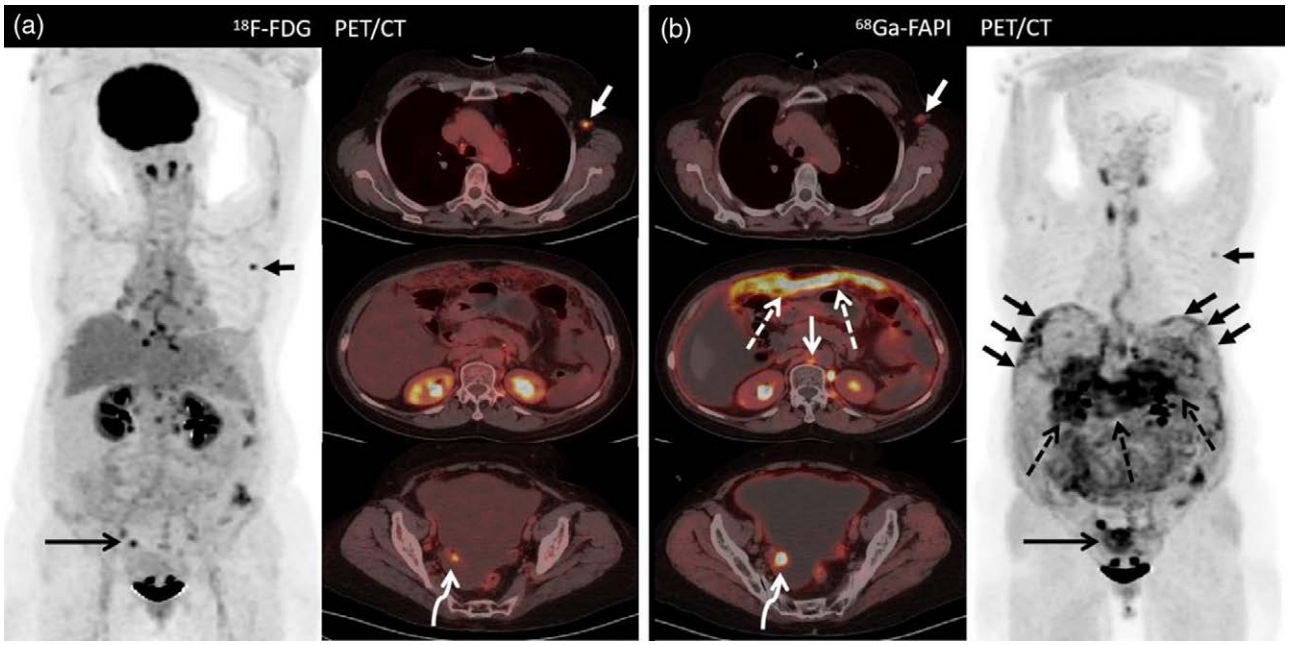

A 55-year-old woman (Patient 2) presenting with abdominal distension and pain for 2 months with adenocarcinoma cells in the peritoneal fluid. (a) ^{18}F-FDG PET/computed tomography (PET/CT) shows intense tracer uptake in lymphadenitis in the left axilla (short arrow; SUVmax, 7.9). Besides this, the thickened peritoneum, mesentery, and multiple nodules indicate low ^{18}F-FDG activity. (b) Besides the slight uptake from left axilla (short arrow; SUVmax, 3.4), images from ^{68}Ga-FAPI PET/CT demonstrate much higher tracer uptake at the peritoneum, mesentery, and omentum metastases (dashed arrows; SUVmax, 10.7) and metastatic lymph nodes at the retroperitoneal site (short arrow; SUVmax, 12.9) and the primary tumor (bent arrow; SUVmax, 13.7). Subsequent biopsy of the peritoneal nodules shows a metastatic ovarian serous carcinoma. ^{18}F-FDG, fluorine-18-fluorodeoxyglucose; ^{68}Ga-FAPI, gallium 68-labeled fibroblast-activation protein inhibitor; SUVmax, maximum standardized uptake values.

results. One of the bone metastases confirmed as osteoarthritis of the appendix of L5 vertebra was misdiagnosed on ^{68}Ga-FAPI PET/CT (participant 24; Fig. 6). We compared the SUVmax of ^{18}F-FDG and ^{68}Ga-FAPI PET/CT found no evidence of a significant difference between those of the bone and visceral metastases (median SUVmax, 6.9 vs. 7.4, respectively; $P=0.14$). However, ^{68}Ga-FAPI PET/CT showed higher SUVmax values in peritoneal and pleural metastases (median SUVmax, 10.1 vs. 7.6, respectively; $P=0.03$), especially in the latter (Fig. 6 and Table 2).

Comparative results for tumor staging or restaging with ^{68}Ga-FAPI PET/computed tomography

Regarding the overall results of ^{68}Ga-FAPI PET/CT among the 21 patients, 4 patients were upstaged compared with ^{18}F-FDG PET/CT is listed in Table 3. Four of the 11 patients (patients 2, 16, 19, and 24) with newly diagnosed disease were upstaged compared with the initial staging. No patient eligible for restaging was downstaged with both ^{18}F-FDG PET/CT and ^{68}Ga-FAPI PET/CT imaging modalities (Table 3).

^{68}Ga-FAPI uptake and characteristics in secondary ovarian malignancies and ovarian tuberculosis

Due to the similar performance of clinical characteristics and morphologic imaging, six patients were confirmed with secondary ovarian malignancies and ovarian tuberculosis. Pathologic examination served as the reference. Among the patients diagnosed with secondary ovarian malignancies, one had gastric signet-ring cell cancer, one had appendix mucinous carcinoma, and the other had cervical adenocarcinoma. ^{18}F-FDG PET/CT missed the

Fig. 4

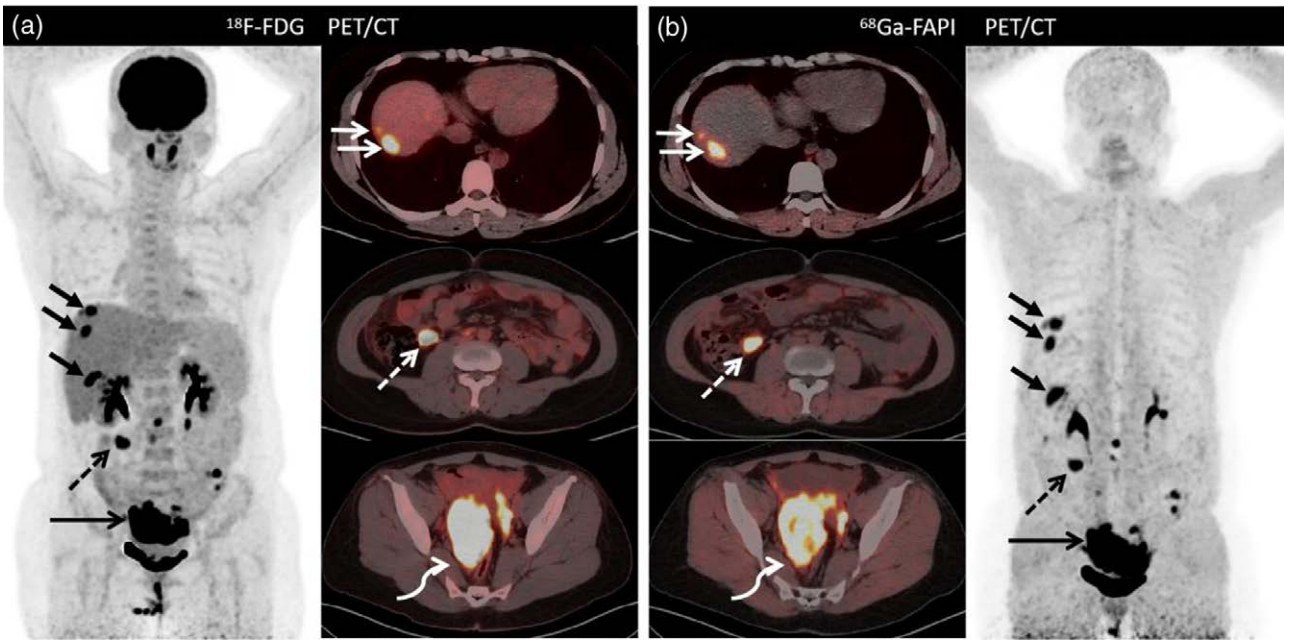

Images of a 44-year-old woman (Patient 26) with known high-grade ovarian carcinoma who underwent ^{18}F-FDG PET/computed tomography for initial staging. Images from both (a) ^{18}F-FDG PET/CT and (b) ^{68}Ga-FAPI PET/CT show intense tracer uptake in the ovarian mass [a, bent arrow (SUVmax, 20.7); b, bent arrow (SUVmax, 13.3)], as well as multiple hepatic nodules [b, solid arrows (SUVmax, 13.8)], [b, solid arrows (SUVmax, 10.0)] and peritoneal metastasis [a, dashed arrow (SUVmax, 17.4); b, dashed arrow (SUVmax, 7.6)]. Nevertheless, the tumor-to-background ratio of ^{68}Ga-FAPI PET was higher than that of ^{18}F-FDG PET. ^{18}F-FDG, fluorine-18-fluorodeoxyglucose; ^{68}Ga-FAPI, gallium 68-labeled fibroblast-activation protein inhibitor; SUVmax, maximum standardized uptake values.

primary tumor located in the gastric wall of the patient with gastric cancer. Nevertheless, ^{68}Ga-FAPI PET/CT showed positive performance in gastric signet-ring cell cancer and appendix mucinous carcinoma, even though ^{18}F-FDG PET/CT missed them. Another three were diagnosed with ovarian tuberculosis. Both ^{18}F-FDG and ^{68}Ga-FAPI uptake was observed around the ovary and inflammatory peritoneum, omentum, and mesentery. However, there was no evidence that ^{68}Ga-FAPI had a higher SUVmax than ^{18}F-FDG PET/CT (2.7 ± 0.4 vs. 2.8 ± 0.3; $P = 0.66$). Moreover, the ^{68}Ga-FAPI uptakes between ovarian malignancies and ovarian tuberculosis revealed that the former show a higher tracer uptake than the latter (median SUVmax, 6.9 vs. 2.6, respectively; $P = 0.03$) (Table 4).

Discussion

^{68}Ga-FAPIs are novel radiotracers that were developed to target the FAP. They demonstrated highly promising results on various tumors in previous studies. ^{68}Ga-labeled FAPIs can be used to visualize the stroma of epithelial neoplasms [14]. This study sought to evaluate the performance of ^{68}Ga-FAPI PET/CT when diagnosing ovarian malignancies with that of ^{18}F-FDG PET/CT and compare the two imaging modalities in the detection of ovarian malignancies. The results of this study demonstrated that, for detecting primary ovarian tumors, ^{68}Ga-FAPI was more sensitive [14 of 14 (100%) vs. 11 of 14 (78%)] than ^{18}F-FDG PET/CT. In some previous studies, different histopathologic types of cancer have been confirmed that lead to no or reduced ^{18}F-FDG uptake, for example, in types of cancer that contain signet-ring and mucinous cells [15,16]. Some of these types of cancers could not be diagnosed accurately on ^{18}F-FDG PET/CT, because of the different glucose metabolic features of target cells. Besides, the ^{18}F-FDG uptake in ovarian is usually variable especially in patients at the reproductive ages because of physiological accumulation and affected by the menstrual cycle [17]. The results of this study revealed ^{68}Ga-FAPI PET/CT could demonstrate different types of ovarian malignancies including HGSC, LGSC, and mucinous carcinoma of the ovarian. Although we were not described whether ^{68}Ga-FAPI had no physiological uptake in the reproductive-age patients, ^{68}Ga-FAPI PET/CT yielded a higher TBR for primary tumor detection in the present study. Thus, ^{68}Ga-FAPI may be as a suitable supplement with ^{18}F-FDG PET/CT.

Lymph node staging is a crucial step for the prognosis and treatment of patients with ovarian malignancies. ^{68}Ga-FAPI PET/CT exhibited more sensitivity in the detection of node metastases compared with ^{18}F-FDG in this study, because more false-negative nodes were not observed on ^{18}F-FDG PET/CT was misdiagnosed. The higher nodal detection rate with ^{68}Ga-FAPI PET/

Fig. 5

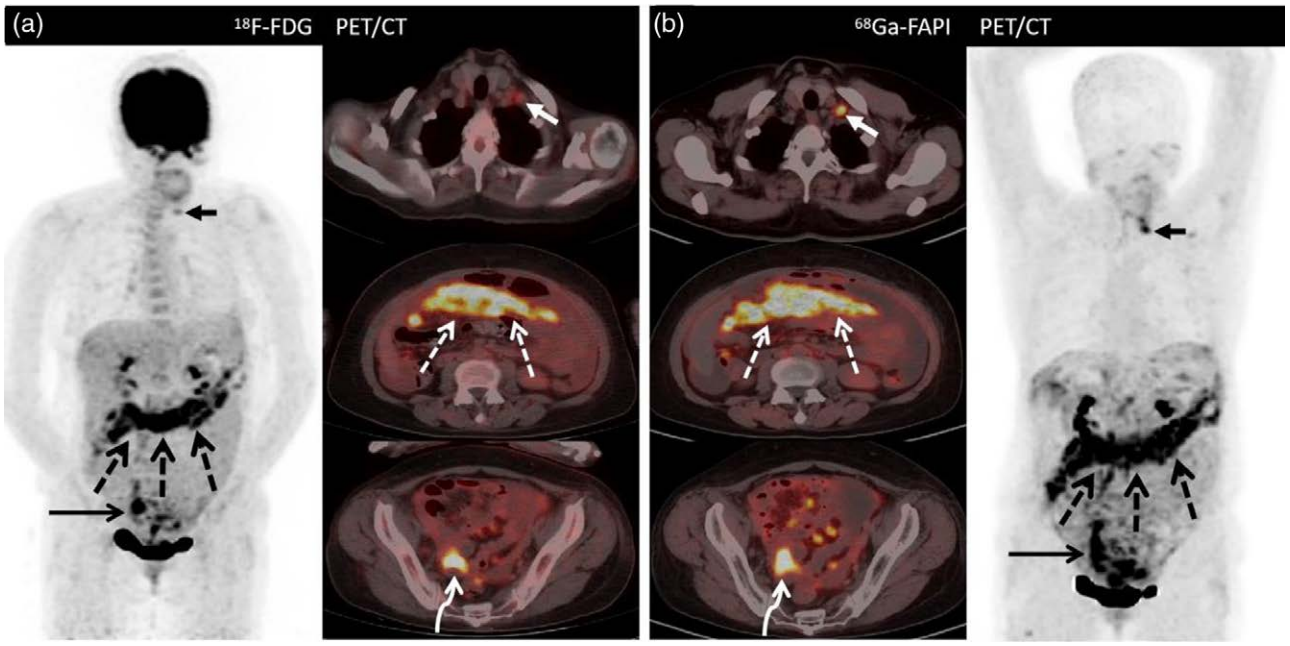

Images of a 51-year-old woman (Patient 13) presenting with abdominal distension and weakness for 1 month, accompanied by rising tumor marker levels. Both ^{18}F-FDG and ^{68}Ga-FAPI PET/CT showed increased tracer uptake in the primary tumor at the pelvic site. (a) Long arrow (SUVmax, 10.4); (b) long arrow (SUVmax, 10.4). Enlarged lymph nodes with tracer uptake in the left neck. a, short arrow (SUVmax, 3.7); b, short arrow (SUVmax, 7.3) and thickened peritoneum, mesentery, and omentum metastases [a, dashed arrow (SUVmax, 9.7]; b, dashed arrow (SUVmax, 9.6)] were detected on both ^{18}F-FDG and ^{68}Ga-FAPI PET/CT. For this patient, ^{18}F-FDG and ^{68}Ga-FAPI PET/CT showed comparative detection efficacy for primary ovarian tumor and lymph node and distant metastases. ^{18}F-FDG, fluorine-18-fluorodeoxyglucose; ^{68}Ga-FAPI, gallium 68-labeled fibroblast-activation protein inhibitor; SUVmax, maximum standardized uptake values.

CT may depend on the higher tracer uptake in different types of ovarian malignancies and lower TBRs, which is consistent with previous studies [10,18,19]. However, ^{68}Ga-FAPI PET/CT was not a more tumor-specific imaging modality than ^{18}F-FDG PET/CT for detecting node metastases [20–22]. For example, one patient exhibited false-positive on both imaging modalities because of lymphadenitis. Nonetheless, ^{68}Ga-FAPI PET/CT may be used as an excellent potential imaging modality when ^{18}F-FDG PET/CT is of limited use.

High-grade ovarian malignancies is prone to the peritoneum, omentum, and mesentery metastases, which are defined as peritoneal carcinomatosis uniformly, the main clinical challenge of advanced-stage ovarian malignancies [4]. In our study, 10 patients had peritoneal carcinomatosis and pleural metastases. However, due to the lower sensitivity of peritoneal carcinomatosis, 3 of the 10 patients were missed on ^{18}F-FDG PET/CT. This may result from peristaltic activity, which often suffers from heterogeneous uptake in the intestinal wall and the small size of the metastases located at the peritoneum, mesentery, and omentum [8,23,24]. Indeed, ^{68}Ga-FAPI demonstrates very low physiological background uptake and unspecific peritoneal uptake in the abdominal cavity, which could be superior to identifying peritoneal carcinomatosis which is similar to the results of previous reports [11,18]. During peritoneal metastasis, tumor-associated fibroblasts (CAF) play important roles in the peritoneal metastasis of ovarian malignancies. The fibroblast activator protein (FAP) is overexpressed in CAF in the tumor microenvironment [25,26]. Consequently, ^{68}Ga-FAPI which targets the fibroblast-activation protein in CAF may exhibit excellent sensitivity to ^{18}F-FDG in the detection of peritoneal carcinomatosis [27]. In addition, fibrosis of peritoneal metastases may also lead to the accumulation of ^{68}Ga-FAPI. Bone and visceral metastases are other common forms of metastasis in ovarian malignancies. In our study, 10 distant metastases were localized to the bone ($n=3$), liver ($n=4$), and spleen ($n=3$). This study found that ^{18}F-FDG PET/CT and ^{68}Ga-FAPI PET/CT did not differ significantly in terms of detection efficacy for bone and visceral metastases in patients with ovarian malignancies. Due to the small number of patients with bone metastases ($n=3$) and visceral metastases ($n=7$), there is challenging to get a definitive explanation. However, previous studies confirm that ^{68}Ga-FAPI is comparable or even more sensitive to ^{18}F-FDG in detecting bone and visceral metastases [28,29]. Therefore, the efficacy evaluation and prognosis monitoring of ovarian malignancies may be visualized using ^{68}Ga-FAPI-PET/CT. Molecular changes in the tumor stroma of ovarian malignancies can be demonstrated in the early stage. Targeting FAP might

Fig. 6

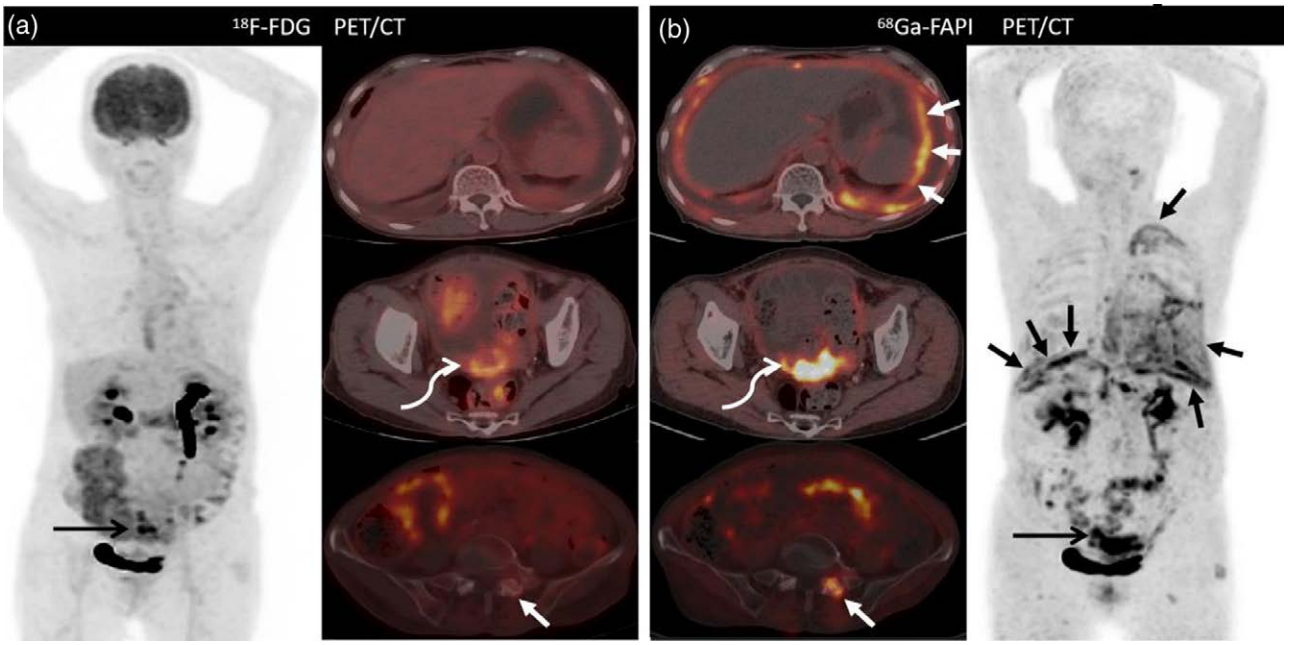

Images of a 76-year-old woman (Patient 24) with known ovarian adenocarcinoma who underwent ^{18}F-FDG PET/computed tomography (PET/CT) for initial staging and presented with chest tightness for 3 months. (a) ^{18}F-FDG PET/CT images show thickened pleura and peritoneum, mesentery, along with a primary tumor with low-to-moderate tracer uptake. (b) Images from ^{68}Ga-FAPI PET/CT show much higher tracer uptake in the thickened pleura (short arrows; SUVmax, 6.5), peritoneum (short arrows; SUVmax, 7.3), and primary tumor (bent arrow; SUVmax, 8.2). Subsequent biopsy of the pleural nodes shows metastatic ovarian carcinoma, and more distant metastasis could be detected using ^{68}Ga-FAPI PET/CT, especially at the pleural and peritoneal sites. However, one of the bone metastases confirmed as osteoarthritis of the appendix of L5 vertebra was misdiagnosed on ^{68}Ga-FAPI PET/CT (short arrow; SUVmax, 4.4). ^{18}F-FDG, fluorine-18-fluorodeoxyglucose; ^{68}Ga-FAPI, gallium 68-labeled fibroblast-activation protein inhibitor; SUVmax, maximum standardized uptake values.

Table 3 Comparison of ^{18}F-FDG and ^{68}Ga-FAPI PET/computed tomography uptake in ovarian malignancies and results for tumor staging/restaging of four patients with ovarian cancer

Participant no.	Age (years)	Diagnosis	Initial staging/ restaging	Tumor stage based on ^{18}F-FDG	Tumor stage based on ^{68}Ga-FAPI	Staging change
2	55	Ovarian cystic adenocarcinoma	Initial staging	IIIA	IIIC	Up
16	57	Ovarian cystic adenocarcinoma	Initial staging	IIIA	IIIC	Up
19	58	Ovarian cystic adenocarcinoma	Initial staging	IIIA	IIIC	Up
24	75	Ovarian cystic adenocarcinoma	Initial staging	IIIC	IVA	Up

^{18}F-FDG, fluorine-18-fluorodeoxyglucose; ^{68}Ga-FAPI, gallium 68-labeled fibroblast-activation protein inhibitor.

present a potential tool for ovarian malignancies with the development of peptide receptor radionuclide therapy.

Three patients diagnosed with ovarian tuberculosis were observed using both ^{68}Ga-FAPI and ^{18}F-FDG PET/CT. The unspecific fibrosis of the lesions located at the peritoneal induced by tuberculosis could also cause positive uptake with ^{68}Ga-FAPI due to the overexpress of FAP. The inflammation would be a principal factor on ^{68}Ga-FAPI PET/CT when explaining the false-positive findings [30–32].

This study has some limitations. First, the number of patients was small ($n = 27$), therefore, no subgroup analyses with histologic classification and BRCA1/2 mutation. Second, the number of different pathologic types of ovarian malignancies was imbalanced. Third, not all the positive lesions were confirmed by histopathologic, due to technical and ethical issues. Consequently, morphologic imaging and follow-up results were also taken as the reference standard in this study.

These results showed that ^{68}Ga-FAPI PET/CT had superior potential than ^{18}F-FDG PET/CT for detecting ovarian tumors, lymph nodes, and peritoneum metastases in patients with ovarian malignancies. Preliminary results regarding ^{68}Ga-FAPI PET/CT as a promising tracer and excellent supplement of ^{18}F-FDG PET/CT for staging and follow-up of ovarian malignancies, as it achieved higher tracer uptake and higher TBRs. Patients

Table 4 Comparison of ^{18}F-FDG and ^{68}Ga-FAPI PET/computed tomography in secondary ovarian malignancies and ovarian tuberculosis

A. Comparison of ^{68}Ga-FAPI PET/CT uptake in secondary ovarian malignancies and ovarian tuberculosis

Index	Ovarian inflammationa (n=3)	Ovarian malignanciesb (n=24)
Median of SUVmax	2.6	6.9
Range of SUV-max	2.3–3.2	2.1–35.8
P value	0.03	

B. Comparison of ^{18}F-FDG and ^{68}Ga-FAPI PET/CT uptake in ovarian tuberculosis

Participant no.	Diagnosis	Indication	^{18}F-FDG uptake of ovarian (mean±SD)	^{68}Ga-FAPI uptake of ovarian (mean±SD)	P value
3/4/9	Ovarian tubercu-losis	Diagnosis	2.8±0.3	2.7±0.4	>0.05

^{18}F-FDG, fluorine-18-fluorodeoxyglucose; ^{68}Ga-FAPI, gallium^{68}-labeled fibroblast-activation protein inhibitor.
[a]Ovarian Inflammation includes three ovarian tuberculosis.
[b]Ovarian malignancies include 1 ovarian mucinous adenocarcinoma, 1 Krukenberg's tumor, 1 appendix mucinous adenocarcinoma, 1 cervical adenocarcinoma, and 20 ovarian cystic adenocarcinomas.

with diabetes can benefit more from ^{68}Ga-FAPI PET/CT. Moreover, FAPI accumulation in the ovaries presented no statistically significant differences between premenopausal and postmenopausal [11]. Consequently, FAPI PET/CT may allow more precise monitoring in ovarian malignancies.

Larger studies and future research are required with more patients to confirm the diagnostic accuracy of ^{68}Ga-FAPI in ovarian malignancies to confirm the usefulness of ^{68}Ga-FAPI PET/CT in ovarian malignancies.

Acknowledgements

The authors gratefully acknowledge all participants.

Guarantors of the integrity of the entire study, all authors; study concepts/study design or data acquisition or data analysis/interpretation, all authors; article drafting or article revision for important intellectual content, all authors; approval of the final version of the submitted article, all authors; agrees to ensure any questions related to the work are appropriately resolved, all authors; literature research, W.Z., L.L., Y.F., L.W., and Y.C.; clinical studies, W.Z., L.L., Y.F., L.W., Y.C.; statistical analysis, W.Z. and Y.F.; and article editing, W.Z. and L.L.

Conflicts of interest

W.Z. supported by the foundation projects from Nuclear Medicine and Molecular Imaging Key Laboratory of Sichuan Province (HYX 18020). For the remaining authors, there are no conflicts of interest.

References

1 Kreeger PK, editor. Clinical staging of ovarian cancer. *Methods Mol Biol* United States,2022; **2424**:3–10.
2 Ledermann JA, Raja FA, Fotopoulou C, Gonzalez-Martin A, Colombo N, Sessa C; ESMO Guidelines Working Group. Newly diagnosed and relapsed epithelial ovarian carcinoma: ESMO clinical practice guidelines for diagnosis, treatment and follow-up. *Ann Oncol* 2013; **24**:vi24–vi32.
3 Lheureux S, Gourley C, Vergote I, Oza AM. Epithelial ovarian cancer. *Lancet* 2019; **393**:1240–1253.
4 Penny SM. Ovarian cancer: an overview. *Radiol Technol* 2020; **91**:561–575.
5 Bar-Shalom R, Yefremov N, Guralnik L, Gaitini D, Frenkel A, Kuten A, *et al*. Clinical performance of PET/CT in evaluation of cancer: additional value for diagnostic imaging and patient management. *J Nucl Med* 2003; **44**:1200–1209.
6 Becker J, Schwarzenböck SM, Krause BJ. FDG PET hybrid imaging. *Recent Results Cancer Res* 2020; **216**:625–667.
7 Marzola MC, Chondrogiannis S, Rubello D. Fludeoxyglucose F 18 PET/CT assessment of ovarian cancer. *PET Clin* 2018; **13**:179–202.
8 Kitajima K, Murakami K, Sakamoto S, Kaji Y, Sugimura K. Present and future of FDG-PET/CT in ovarian cancer. *Ann Nucl Med* 2011; **25**:155–164.
9 Kratochwil C, Flechsig P, Lindner T, Abderrahim L, Altmann A, Mier W, *et al*. (68)Ga-FAPI PET/CT: tracer uptake in 28 different kinds of Cancer. *J Nucl Med* 2019; **60**:801–805.
10 Chen H, Pang Y, Wu J, Zhao L, Hao B, Wu J, *et al*. Comparison of [(68)Ga]Ga-DOTA-FAPI-04 and [(18)F] FDG PET/CT for the diagnosis of primary and metastatic lesions in patients with various types of cancer. *Eur J Nucl Med Mol Imaging* 2020; **47**:1820–1832.
11 Dendl K, Koerber SA, Finck R, Mokoala K, Staudinger F, Schillings L, *et al*. (68)Ga-FAPI-PET/CT in patients with various gynecological malignancies. *Eur J Nucl Med Mol Imaging* 2021; **48**:4089–4100.
12 Lindner T, Loktev A, Altmann A, Giesel F, Kratochwil C, Debus J, *et al*. Development of quinoline-based theranostic ligands for the targeting of fibroblast activation protein. *J Nucl Med* 2018; **59**:1415–1422.
13 Boellaard R, Delgado-Bolton R, Oyen WJ, Giammarile F, Tatsch K, Eschner W, *et al*.; European Association of Nuclear Medicine (EANM). FDG PET/CT: EANM procedure guidelines for tumour imaging: version 2.0. *Eur J Nucl Med Mol Imaging* 2015; **42**:328–354.
14 Sharma P, Singh SS, Gayana S. Fibroblast activation protein inhibitor PET/CT: a promising molecular imaging tool. *Clin Nucl Med* 2021; **46**:e141–e150.
15 Strobel O, Büchler MW. Pancreatic cancer: FDG-PET is not useful in early pancreatic cancer diagnosis. *Nat Rev Gastroenterol Hepatol* 2013; **10**:203–205.
16 Dondi F, Albano D, Giubbini R, Bertagna F. 18F-FDG PET and PET/CT for the evaluation of gastric signet ring cell carcinoma: a systematic review. *Nucl Med Commun* 2021; **42**:1293–1300.
17 Wang Q, Yang S, Tang W, Liu L, Chen Y. (68)Ga-DOTA-FAPI-04 PET/CT as a promising tool for differentiating ovarian physiological uptake: preliminary experience of comparative analysis with (18)F-FDG. *Front Med (Lausanne)* 2021; **8**:748683.
18 Pang Y, Zhao L, Luo Z, Hao B, Wu H, Lin Q, *et al*. Comparison of (68)Ga-FAPI and (18)F-FDG uptake in gastric, duodenal, and colorectal cancers. *Radiology* 2021; **298**:393–402.
19 Wang H, Zhu W, Ren S, Kong Y, Huang Q, Zhao J, *et al*. (68)Ga-FAPI-04 versus (18)F-FDG PET/CT in the detection of hepatocellular carcinoma. *Front Oncol* 2021; **11**:693640.
20 Giesel FL, Kratochwil C, Schlittenhardt J, Dendl K, Eiber M, Staudinger F, *et al*. Head-to-head intra-individual comparison of biodistribution and tumor uptake of (68)Ga-FAPI and (18)F-FDG PET/CT in cancer patients. *Eur J Nucl Med Mol Imaging* 2021; **48**:4377–4385.
21 Lan L, Zhang S, Xu T, Liu H, Wang W, Feng Y, *et al*. Prospective comparison of (68)Ga-FAPI versus (18)F-FDG PET/CT for tumor staging in biliary tract cancers. *Radiology* 2022; **304**:648–657.
22 Lan L, Liu H, Wang Y, Deng J, Peng D, Feng Y, *et al*. The potential utility of [(68) Ga]Ga-DOTA-FAPI-04 as a novel broad-spectrum oncological and non-oncological imaging agent-comparison with [(18)F]FDG. *Eur J Nucl Med Mol Imaging* 2022; **49**:963–979.
23 Kemppainen J, Hynninen J, Virtanen J, Seppänen M. PET/CT for evaluation of ovarian cancer. *Semin Nucl Med* 2019; **49**:484–492.
24 Soussan M, Des Guetz G, Barrau V, Aflalo-Hazan V, Pop G, Mehanna Z, *et al*. Comparison of FDG-PET/CT and MR with diffusion-weighted imaging for assessing peritoneal carcinomatosis from gastrointestinal malignancy. *Eur Radiol* 2012; **22**:1479–1487.
25 Lai D, Ma L, Wang F. Fibroblast activation protein regulates tumor-associated fibroblasts and epithelial ovarian cancer cells. *Int J Oncol* 2012; **41**:541–550.
26 Li M, Cheng X, Rong R, Gao Y, Tang X, Chen Y. High expression of fibroblast activation protein (FAP) predicts poor outcome in high-grade serous ovarian cancer. *BMC Cancer* 2020; **20**:1032.

27 Mhawech-Fauceglia P, Yan L, Sharifian M, Ren X, Liu S, Kim G, *et al*. Stromal expression of fibroblast activation protein alpha (FAP) predicts platinum resistance and shorter recurrence in patients with epithelial ovarian cancer. *Cancer Microenviron* 2015; **8**:23–31.
28 Şahin E, Elboğa U, Çelen YZ, Sever ON, Çayırlı YB, Çimen U. Comparison of (68)Ga-DOTA-FAPI and (18)FDG PET/CT imaging modalities in the detection of liver metastases in patients with gastrointestinal system cancer. *Eur J Radiol* 2021; **142**:109867.
29 Wu J, Wang Y, Liao T, Rao Z, Gong W, Ou L, *et al*. Comparison of the relative diagnostic performance of [(68)Ga]Ga-DOTA-FAPI-04 and [(18)F]FDG PET/CT for the detection of bone metastasis in patients with different cancers. *Front Oncol* 2021; **11**:737827.
30 Chen H, Zhao L, Ruan D, Pang Y, Hao B, Dai Y, *et al*. Usefulness of [(68)Ga]Ga-DOTA-FAPI-04 PET/CT in patients presenting with inconclusive [(18)F]FDG PET/CT findings. *Eur J Nucl Med Mol Imaging* 2021; **48**:73–86.
31 Zheng J, Lin K, Zheng S, Yao S, Miao W. 68Ga-FAPI and 18F-PET/CT images in intestinal tuberculosis. *Clin Nucl Med* 2022; **47**:239–240.
32 Alçın G, Tatar G, Şahin R, Baloğlu MC, Çermik TF. Peritoneal tuberculosis mimicking peritoneal carcinomatosis on 68 Ga-FAPI-04 and 18 F-FDG PET/CT. *Clin Nucl Med* 2022; **47**:e557–e558.